EUROfusion

EUROFUSION WPMAG-REP(16) 16566

R. Zanino et al.

Common approach for thermal-hydraulic calculations

REPORT

This work has been carried out within the framework of the EUROfusion Consortium and has received funding from the Euratom research and training programme 2014-2018 under grant agreement No 633053. The views and opinions expressed herein do not necessarily reflect those of the European Commission.

MEMO for WPMAG-MCD-2.1

Task Area:	**MCD-2.1**	
Deliverable:	**D01**	
Title:	**Common approach for thermal-hydraulic calculations**	
IDM Reference:	EFDA_D_2LMECE	
Authors:	L. Savoldi, R. Zanino	
Date:	16/09/2016	
Version	1.2	
Abstract:	The document combines the previous several different versions of "common approaches" for the thermal-hydraulic and quench calculations. The purpose of this document is to serve as common guideline for the TF WP design and analyses to be performed in the year 2016 and beyond. This memo is complemented by a detailed technical memo dealing with the common operating values for DEMO magnets design [1]. ----------	
Distribution list:	R. Bonifetto, P. Bruzzone, M. Coleman, B. Lacroix, M. Lewandowska, L. Muzzi, L. Savoldi, K. Sedlak, R. Vallcorba, L. Zani, R. Zanino	
Reviewers	**Name**	**Role**
	P. Bruzzone	WPMAG WGC
	M. Coleman	WPMAG PMU RO
Approver	L. Zani	WPMAG PL

Table of Contents

1 Acronyms and abbreviations

The acronyms and abbreviations used in this report are collected in Table I.

Table I – Acronyms and abbreviations

Acronym	Description	Units
A	Area	[m^2]
B	Bundle	-
CC	Cooling channel	-
C_F	Drag coefficient	[m^{-1}]
CICC	Cable-in-conduit conductor	-
CEA	Commissariat à l'énergie atomique	-
CFD	Computational fluid dynamics	-
CS	Central Solenoid	-
D	Diameter	[m]
f	Friction factor	-
g	Gap	[m]
HTC	Heat transfer coefficient	[W/m^2K]
in	Inner	-
IPPLM	Institute of Plasma Physics and Laser Microfusion	-
K	Permeability	[m^2]
Nu	Nusselt number	-
out	Outer	-
PoliTo	Politecnico di Torino	-
Pr	Prandtl number	-
R_{th}	Thermal resistance	[m^2K/W]
q"	Heat flux	[W/m^2]
Re	Reynolds number	-
RU	Research unit	-
sp	Spiral	-
SPC	Swiss Plasma Center	-
T	Temperature	[K]
t	thickness	[m]
TH	Thermal-Hydraulic	-
TF	Toroidal Field	-
w	Width	[m]
WP	Winding Pack	-
WP#1	Winding Pack (SPC design)	-
WP#2	Winding Pack (ENEA design)	-
WP#3	Winding Pack (CEA design)	-
α	Rectangle aspect ratio	-
δ	Thickness	[m]
φ	Void fraction	-

2 Introduction

The purpose of this document is to serve as common guideline for the TF WP design and analyses to be performed in the year 2016 and beyond.

The document combines the previous several different versions of "common approaches" for the TH and quench calculations [2, 3]. It is mainly based on the discussion and conclusions in the memo "Common approach for burn studies" [4].

It summarizes the common approach agreed for TH analyses to be done by several RUs on DEMO TF conductors, defining in particular:

- the friction factor for the bundle (B) region and for the cooling channels (CCs)
- the different heat transfer coefficients
- the model for the heat transfer between B and CCs
- a recommendation for the modelling of the thermal coupling between neighbouring turns, layers or pancakes
- a recommendation for the modelling of the thermal coupling between WP and casing.

This memo is complemented by a detailed technical memo dealing with the common operating values for DEMO TF WP design [1].

3 Definitions

The definition of the wetted perimeter(s), of the hydraulic diameter(s) and of the flow area(s) adopted by each RU should be clearly defined in its deliverables.

4 Fanning friction factor correlations

The correlations reported in this section are mainly taken from [5]. In the present document, the Fanning friction factor f for any He channel is defined as:

$$f = -\frac{D_H}{2\rho v^2}\frac{dp}{dx} = -\frac{D_H \rho \left(A_{flow}\right)^2}{2\dot{m}^2}\frac{dp}{dx} \tag{1}$$

where dp/dx is the pressure gradient along the channel, D_H is the hydraulic diameter of the channel, v is the average fluid speed in the channel, ρ is the density, $\dot{m}$ is the mass flow rate and A_{flow} the flow area.

4.1 Bundle region

The correlation based on the Darcy-Forchheimer equation for the flow in porous media [6, 7, 8], [9], is recommended as the primary correlation to be used in TH simulations. The friction factor correlation resulting from the Darcy–Forchheimer equation can be written as:

$$f = \frac{D_h^2 \varphi}{2K} \frac{1}{\mathrm{Re}} + \frac{D_h \varphi^2}{2} \frac{C_F}{\sqrt{K}} \tag{2}$$

where D_h is the hydraulic diameter, φ is the void fraction, *Re* is the Reynolds number, C_F is the drag coefficient that characterize a specific porous medium and *K* is the permeability. :
The drag coefficient can be defined as [7]:

$$\frac{C_F}{\sqrt{K}} = \frac{2.42}{\varphi^{5.80}} \ [\mathrm{m}^{-1}] \tag{3}$$

while for the permeability a formulation is available [7]:

$$K = 19.6 \cdot 10^{-9} \frac{\varphi^3}{(1-\varphi)^2} \ [\mathrm{m}^2] \tag{4}$$

where it should be noted, however, that this dependence on porosity only cannot be too realistic, since it is expected that *K* should depend also on the tortuosity of the flow path and therefore, in the case of a CICC, on the different cabling twist pitches. Note however that a friction factor correlation taking into account the tortuosity of the flow path does not exist yet (only the dependence on the cabling pattern - braided vs. non-braided conductors - was investigated so far in [10]).

4.2 Cooling channel(s) region

For WP#1 (SPC conductors featuring 2 equilateral triangle ducts and 1 rectangular duct [11], see Figure 1), the recommended references in the case of laminar flow (Re < 2000) are the classical smooth tube correlations:

- for the equilateral-triangle ducts

$$f_{lam-tri} = \frac{13.33}{\mathrm{Re}_{tri}} \tag{5}$$

  where the Reynolds number Re_{tri} is defined using $D_h = L/\sqrt{3}$ (being *L* the triangle side) [12] as characteristic length. A_{flow} in (5) is defined as $\sqrt{3}\mathrm{L}^2/4$.

- for the rectangular duct with dimensions $2a \times 2b$ ($b < a$), $\alpha = b/a$,

$$f_{lam-rec} = \frac{24\left(1 - 1.3553\alpha + 1.9467\alpha^2 - 1.7012\alpha^3 + 0.9564\alpha^4 - 0.2537\alpha^5\right)}{\mathrm{Re}_{rec}} \tag{6}$$

  where the Reynolds number Re_{rec} is defined using $D_h = 4ab/(a + b)$ as characteristic length. A_{flow} in (6) is defined as $2a \times 2b$.

For the turbulent flow in smooth circular and non-circular ducts the following Bhatti-Shah correlation (accuracy ±2%) is recommended [13]:

$$f_{turb} = 0.00128 + 0.1143\,\mathrm{Re}^{-0.311}, \text{ valid for } 4000 < \mathrm{Re} < 10^7 \tag{7}$$

where the Reynolds number is Re_{tri} and Re_{rec} in the triangular and rectangular ducts, respectively.
In the transition regime, i.e. for 2000 < Re < 4000, it is suggested to linearly interpolate between laminar and turbulent values at Re = 2000 and Re = 4000, respectively.

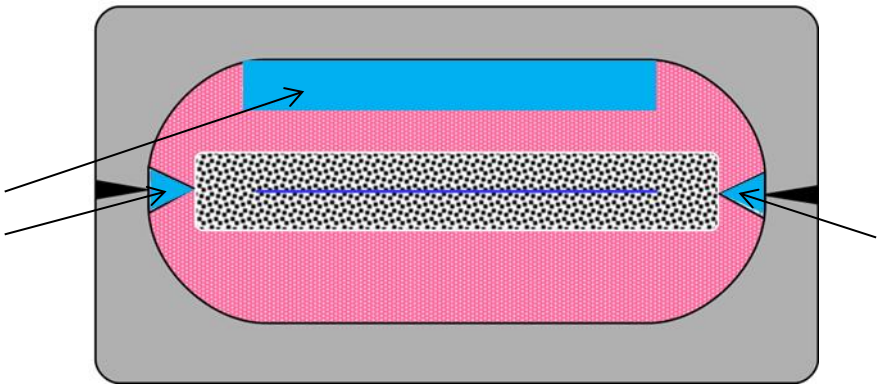

Figure 1. WP#1 conductor foreseen for DL1 (reproduced from [11]). The He cooling channels are coloured in light blue and pointed to with arrows; grey colour indicates the steel jacket, magenta colour the copper mixed matrix, checked area the bundle of superconducting strands.

For WP#2 (ENEA conductor featuring two CCs delimited by a spiral [14], see Figure 2) the use a predictive friction factor correlation proposed in [15] in the following implicit form is recommended:

$$R(h^+) = \sqrt{\frac{2}{f}} + 2.5\ln\left(\frac{2t_{sp}}{D_{in}}\right) + 3.75\,, \tag{8}$$

$$h^+ = \frac{t_{sp}}{D_{in}}\mathrm{Re}\sqrt{f/2}\,, \tag{9}$$

$$R(h^+) = \alpha\left(h^+\right)^{\beta}\left(\frac{g_{sp}}{t_{sp}}\right)^{\gamma}\,, \tag{10}$$

where t_{sp} is the spiral height (thickness), g_{sp} is the spiral gap width, and the inner spiral diameter D_{in} is used as a reference dimension in the evaluation of the Re. The function given by (9-11) was tested in [15] using the friction factor vs. *Re* data resulting from the pressure drop measurements on a pipe with different spiral inserts. Three spirals with the same height (t_{sp} = 1 mm), similar D_{in}/D_{out} of about 10/12 mm, similar strip width (w_{sp} = 6.2 to 6.5 mm) and different gap width (g_{sp} = 2.4 to 5.3 mm) were used in experimental tests in [15]. It was found that the best fit to all data considered was obtained for:

$$\alpha = 11.88,\ \beta = 0.039 \text{ and } \gamma = -0.299. \tag{11}$$

Later work based on the CFD simulations of flow in the central channel of D_{in} = 7 mm [16] provided the following values of parameters α, β and γ in (11):

$$\alpha = 6.4,\ \beta = 0.1717 \text{ and } \gamma = -0.3428. \tag{12}$$

In any case, Eqs. 9-11 are valid in the range 5e4 < *Re* < le6.

In case of laminar regime (Re < 2000), it is proposed to stick to the classical smooth tube correlation for circular ducts:

$$f^* = \frac{16}{\mathrm{Re}}, \tag{13}$$

considering the spiral thickness like an artificial roughness of the inner surface of the pipe, which cannot be "seen" when the boundary layer occupies the entire tube cross section, while in the region 2000 < Re < 5e4 it is proposed to just linearly interpolate between the laminar and turbulent values.
A_{flow} in (2) is defined $\pi D_{in}^2/4$.

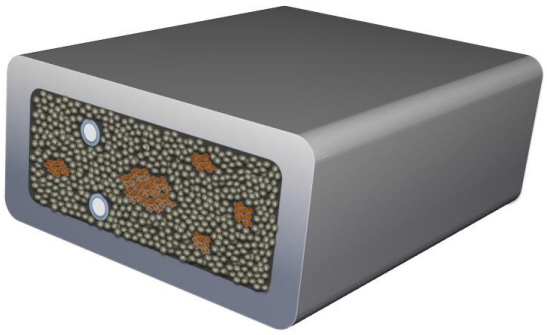

Figure 2. WP#2 conductor.

For WP#3 (CEA ITER-type CICC featuring a single CC delimited by spiral [17], see Figure 3), an experimental fit corresponding to a spiral with 8/10 mm inner/outer diameters and void fraction around 20 to 30 % is proposed as a reference:

$$f_{spiral} = \frac{0.42}{4 \cdot \mathrm{Re}^{0.1}} \tag{14}$$

where Re is computed using D_{out} as characteristic length.
This correlation, which is independent on the spiral width and pitch as a main difference to the recipe proposed in Eqs. 9-11, was established from measurements on several spirals for ITER TF and CS conductors [18, 19].
A_{flow} in (2) in this case is defined as $\pi D_{out}^2/4$.

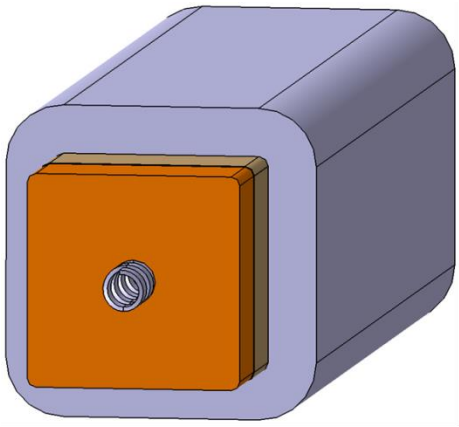

Figure 3. WP#3 conductor (reproduced from [17]).

5 Heat transfer coefficient (HTC) correlations

Three different HTCs are described in this section:

- between He and strands, jacket and the wall of CC(s)
- between He in the B and He in the CC(s)
- between strands and jacket (contact).

5.1 HTC between He and strands, jacket and the wall of CC(s)

According to the standard boundary layer theory [12], in the thermal (sub-)layer at the wall (coincident with the laminar sub-layer for $Pr = 1$) the heat transfer between the solid wall and the fluid occurs only by conduction since the fluid is stagnant at the wall. When the *Re* of the fluid is small enough that no turbulent boundary layer is present, then the *Nu* should reduce to a minimum constant value that corresponds to pure conduction in the laminar boundary layer (Nu_{laminar}).

In all geomtries, the value of Nu_{laminar} is slightly different for the two cases of heat transfer from a wall at constant temperature ($Nu_{\text{T,laminar}}$) or from a wall at constant heat flux ($Nu_{\text{flux,laminar}}$). The average value among these two options, none of which is fully relevant for the situation at hand, is recommended. More in detail:

1. In smooth circular tubes $Nu_{T,laminar,circ} = 3.66$ and $Nu_{flux,laminar,circ} = 4.36$ [12], giving:

$$Nu_{laminar,circ} = 4.01 \tag{15}$$

2. In equilateral triangle ducts, $Nu_{T,laminar,tri} = 2.47$ and $\text{Nu}_{flux,laminar,tri} = 1.892$ [13], giving:

$$\text{Nu}_{laminar,tri} = 2.181 \tag{16}$$

3. In rectangular ducts with dimensions $2a \times 2b$ ($b < a$) and $\alpha = 2b/2a$, for Nu_{laminar} it is recommended to use the average of:

$$Nu_{T,laminar,rect} = 7.541 \cdot (1 - 2.610\,\alpha + 4.970\,\alpha^2 - 5.119\,\alpha^3 + 2.702\,\alpha^4 - 0.548\,\alpha^5) \quad (17)$$

and

$$Nu_{flux,laminar,rect} = 8.235 \cdot (1 - 10.6044\alpha + 61.1755\,\alpha^2 - 155.1803\alpha^3 + 176.9203\alpha^4 - + 176.9203\alpha^4 - 72.9236\alpha^5) \quad (18)$$

both taken from [13].

When the *Re* of the fluid is large enough that a turbulent boundary layer is present, the standard Dittus-Boelter correlation can be used *in any type of ducts and bundles*, and to a good approximation both for the uniform surface temperature and heat flux conditions*:*

$$Nu_{turbulent} = 0.023\,Re^{0.8}\,Pr^{y} \quad (19)$$

y at the exponent of *Pr* should be taken as 0.4 when the wall is hotter than the fluid and 0.3 when the wall is colder than the fluid. Eq. (20) has been experimentally confirmed in the range $0.6 < Pr < 160$ and $Re > 10000$, for small to moderate temperature differences and properties evaluated at the average wall/bulk temperature.

The recommended value for the overall *Nu* to be retained in the simulations is then:

$$Nu = \max\,(Nu_{laminar}\,,\,Nu_{turbulent}). \quad (20)$$

It is recommended *not* to rely on heat-momentum transfer (so-called Colburn) analogies, which, as far as momentum transfer is concerned, are only valid if there is no form drag [20, pp. 516-520]. In the particular case of the ITER CICC central channel this point was also clearly confirmed by detailed CFD simulations [21].

5.2 HTC between He in the B and He in the CC(s)

The flux repartition between perforated and non-perforated area is taken into account as follows:

$$h_{global} = h_{open} \times perfor + h_{closed} \times (1 - perfor), \quad (21)$$

being *perfor* the fraction of perforated area. As a first simplified approach, and in the lack of experimental data to develop suitable correlations at this level of detail, the different contributions to (22) can be computed as:

$$h_{open} = \frac{1}{\frac{1}{h_B} + \frac{1}{h_C}} \quad (22)$$

$$h_{closed} = \frac{1}{\frac{D_{ave}}{D_{out}h_B} + \frac{D_{ave}}{2k_{steel}}\ln\left(\frac{D_{out}}{D_{in}}\right) + \frac{D_{ave}}{D_{in}h_C}} \tag{23}$$

where D_{ave} is the average spiral diameter $(D_{in}+D_{out})/2$, h_B and h_C are the HTC between the He in B and the wall of the CC and between the He in the CC and the wall of the CC, respectively. In the case of h_{open} the perturbation introduced in h_B and h_C by the presence of a permeable wall is neglected.
The thermal conductivity k_{steel} is evaluated at the tube temperature, considered equal to the average of the He temperatures in the two hydraulic channels (B and CC).

The general recipe in (22) should be applicable to all the different conductors considered here, suitably defining the parameter *perfor* to model the actual topology of the bundle/cooling channels interface of the different WP conductors, see the RUs deliverables for details.

5.3 HTC between strands and jacket

The contact HTC between the strands and the jacket is difficult to model properly. Historically it was assumed constant and equal to 500 W/m^{2}K [22]. The contact area between the strands and the jacket strongly depends on the conductor design and should be specified by each RU in the deliverable where the analysis is presented.

6 Thermal coupling between turns, layers, pancakes

The inter-turn/inter-layer/inter-pancake thermal coupling has been proven to play a non-negligible role in [23, 24, 25, 26] and thus its implementation is encouraged.
A possible strategy to account for the inter-turn/inter-layer/inter-pancake thermal coupling is the one adopted in the 4C code [27], described here.
The (minimum) thermal resistance (1/HTC) between different turns/layers/pancakes is computed as

$$R_{th} = \frac{\delta}{k} \tag{24}$$

where k is the thermal conductivity of the insulation material between turns/layers/pancakes and δ is the thickness of the insulation layer. In case of multi-layer insulation the total thermal resistance should be computed as a series of the thermal resistances of each layer. These recipes provide a lower bound for the total thermal resistance since the contact resistances are neglected. The resulting heat flux between the jacket (at temperature $T(x)$) of the two neighbouring turns/layers/pancakes i and j is then

$$q'' = \frac{\left(T_i(x) - T_j(x)\right)}{R_{th}}. \tag{25}$$

Both the insulation material (and in particular its thermal conductivity) and the value of δ depend on the WP design. The thermal conductivity is evaluated at the mean temperature between $T_i(x)$ and $T_j(x)$.

7 Thermal coupling between WP and casing

The amount of heat transferred, between the WP and the casing strongly depends on the casing cooling channels (CCC) design, which has started very recently [28] [29], [30]. The use of a model including both the WP and the casing is encouraged.
In any case, one of the aims of the CCC design should be to take care completely of the NH load on the casing. If that is achieved [28], [29], [30], it can then be assumed that there is no heat transfer from the TF case to the TF WP. However, for the same casing cooling design the results strongly depend on the material thermal conductivity as well as on the coupling between the casing cooling channels and the casing itself. The investigation of this topic is encouraged.

8 Conclusions

Correlations were provided for all actors to be applied to their TH activities associated to the respective WP designs.
The present document can/will be revised periodically according to the evolutions of both design and common views of MCD-2.2 actors on the subject.

9 Acknowledgements

The authors thank K. Sedak, M. Lewandowska and B. Lacroix for their contributions and comments.

References

[1] K. Sedlak, “Common operating values for DEMO Magnet design for 2016,” EFDA_D_2MMDTG, v1.2, 22/03/2016.

[2] R. Bonifetto, B. Lacroix, M. Lewandowska, L. Savoldi, K. Sedlak, R. Vallcorba and R. Zanino, “Proposal of common approaches for quench analyses,” EFDA_D_2JP3JR, 02/02/2015.

[3] B. Lacroix and R. Vallcorba, “Common approach for quench analyses,” EFDA_D_2M6DW4 , 28/01/2016.

[4] R. Bonifetto, B. Lacroix, M. Lewandowska, L. Savoldi, K. Sedlak, R. Vallcorba and R. Zanino, “Proposal of scaling laws for thermal-hydraulic analyses in normal operating conditions.,” EFDA_D_2LCLKZ, 08/01/2015.

[5] M. Lewandowska, “Review of the friction factor correlations for the bundle region of CICC,” WPMAG-MCD-2.1-T01C, EFDA_D_2MGRLB, v.1.0.

[6] L. Bottura and C. Marinucci, “A Porous Medium Analogy for the Helium Flow in CICC’s,” *Int. J. Heat Mass Transfer,* vol. 51, p. 2494–2505, 2008.

[7] M. Bagnasco, L. Bottura and M. Lewandowska, “Friction factor correlation for CICC’s based on a porous media analogy,” *Cryogenics,* vol. 50, p. 711–719, 2010.

[8] R. Zanino and L. Savoldi Richard, “A review of thermal-hydraulic issues in ITER cable-in-conduit conductors,” *Cryogenics,* vol. 46, pp. 541-555, 2006.

[9] M. Lewandowska, “Friction factor correlations for the bundle region of CICC,” EFDA_D_2KZA7D, 26/11/2014.

[10] M. Lewandowska and M. Bagnasco, “Modified friction factor correlation for CICC’s based on a porous media analogy,” *Cryogenics,* vol. 51, pp. 541-545, 2011.

[11] K. Sedlak, “TF conductor and WP#1 design based on 2015 reference,” EFDA_D_2MHQQ5, 11/01/2016.

[12] F. Incropera and D. Dewitt, Fundamentals of heat and mass transfer, 6th edition: John Wiley & Sons, 2006.

[13] R. Shah and D. Sekulić, Fundamentals of Heat Exchanger Design, New Jersey: Wiley, 2003.

[14] L. Muzzi, S. Turtù, C. Fiamozzi Zignani and A. Anemona, “Design of 2015 TF Winding Pack Option 2 (WP#2) and of “ENEA” LTS cable,” EFDA_D_2LF3Z8, 26/11/2015.

[15] R. Zanino, P. Santagati, L. Savoldi Richard, A. Martinez and S. Nicollet, “Friction factor correlation with application to the central cooling channel of cable-in-conduit superconductors for fusion magnets,” *IEEE Transactions on Applied Superconductivity,* vol. 10, pp. 1066-1069, 2000.

[16] R. Zanino, S. Giors and L. Savoldi Richard, “CFD modeling of ITER cable-in-conduit superconductors. Part III: correlation for the central channel friction factor,” *Proceedings of the 21th International Cryogenic Engineering Conference (ICEC21),* vol. 1, p. 207, 2007.

[17] D. Ciazynski and A. Torre, “TF WP#3 design based on 2015 EUROfusion configuration,” EFDA_D_2MDLUL, 09/10/2015.

[18] S. Nicollet, D. Bessette, H. Cloez, P. Decool, B. Lacroix, C. Lebailly and J. Serries, “Review of singular cooling inlet and linear pressure drop for ITER Coils Cable In Conduit Conductor,” *AIP Conference Proceedings,* vol. 823, pp. 1757-1764, 2006.

[19] “SSA-16, Deliverable 2.1: Pressure Drop Measurements on first CS Conductor and 3 central Spirals,” CEA report, 2014.

[20] R. Brodkey and H. Hershey, Transport Phenomena: A Unified Approach, McGraw-Hill, 1988.

[21] R. Zanino and S. Giors, “CFD modeling of ITER cable-in-conduit superconductors. Part V: combined momentum and heat transfer in rib roughened pipes,” *Advances in Cryogenic Engineering,* vol. 53, pp. 1261-8, 2008.

[22] N. Koizumi, T. Takeuchi and K. Okuno, “Development of advanced Nb3Al superconductors for a fusion demo plant,” *Nuclear Fusion,* vol. 45, pp. 431-438, 2005.

[23] L. Savoldi, R. Bonifetto, L. Muzzi and R. Zanino, “Analyses of low- and high-margin Quench Propagation in the European DEMO TF Coil Winding Pack,” *IEEE Transactions on Plasma Science,* vol. 44, no. 9, pp. 1564-1570, 2016.

[24] R. Bonifetto, B. Lacroix, L. Savoldi, R. Vallcorba and R. Zanino, “Comparison between

4C and THEA on the analysis of DAS01-WP13 ENEA conductor in normal operating conditions, including nuclear heating," 02/02/2015.

[25] R. Bonifetto, L. Savoldi and R. Zanino, "Results of 4C thermal-hydraulic analysis of WP#2 2014 conductor in normal operating conditions, including nuclear heating," EFDA_D_2AS693, 02/02/2015.

[26] R. Bonifetto, B. Lacroix, L. Savoldi, R. Vallcorba and R. Zanino, "Comparison between 4C and THEA on the analysis of DAS01-WP13 ENEA conductor during quench and 4C thermal-hydraulic analysis of WP#2 2014 during quench," WPMAG- MCD-2.2-T02, EFDA_D_2LAYMB, 13/02/2015.

[27] L. Savoldi Richard and R. Zanino, "M&M: multi-conductor mithrandir code for the simulation of thermal-hydraulic transients in super-conducting magnets," *Cryogenics*, vol. 40, pp. 179-189, 2000.

[28] R. Zanino, R. Bonifetto, L. Muzzi, O. Dicuonzo, G. F. Nallo, L. Savoldi and S. Turtù, "Development of a Thermal-Hydraulic Model for the European DEMO TF Coil," *IEEE Transactions on Applied Superconductivity*, vol. 26, no. 3, p. 4201606, 2016.

[29] F. Nunio, "Thermal analyses on TF system," WPMAG-MCD-3.2-T001-D001, EFDA_D_2MZ7PC, v.1.0, May 12, 2016.

[30] R. Vallcorba, B. Lacroix, D. Ciazynski, A. Torre, F. Nunio, L. Zani, Q. Le Coz, M. Lewandowska and M. Coleman, "Thermo-hydraulic analyses associated with a CEA design proposal for a DEMO TF conductor," *to appear in Cryogenics*, 2016.